Lithuanian Journal of Physics
Vol. **63**, No. 1, pp. 15–24 (2023)

ISSN 1648-8504 eISSN 2424-3647
DOI: https://doi.org/10.3952/physics.2023.63.1.3

PHYSICAL-AND-CHEMICAL PROCESSES AT THE INTERFACES OF (Cu–Ni–Mn–Fe)/(W–C) COMPOSITES

O.V. Sukhova

Department of Engineering Mechanics and Energy Systems, Institute of Transport Systems and Technologies, National Academy of Sciences of Ukraine, 5 Pisarzhevsky St., 49005 Dnipro, Ukraine
Email: sukhovaya@ukr.net

Received 16 July 2022; accepted 18 January 2023

The spontaneous infiltration method for fabricating composites was used, in which molten Cu–Ni–Mn–Fe binders penetrated W–C filler particles due to capillary forces. The metal matrix composites thus obtained were characterized for phase composition, microstructure, porosity and microhardness. All composites were studied in their as-prepared condition with further annealing at 900°C for 60 and 750 h. It was shown that the mechanism based on the dissolution/diffusion bonding of the particulate/matrix interface was in agreement with the results of this study. The interfacial reactions provided a driving force for wetting but did not give rise to unwanted phases that could degrade the properties of the composite materials. From the EDX measurements it was concluded that mainly Fe atoms diffused from the Cu–Ni–Mn–Fe binders into the WC phase of the eutectic (WC+W_2C) filler. Dissolution of this phase resulted in the appearance of W_2C layer at the interface. Annealing at 900°C significantly promoted the interfacial reaction especially during the first 60 h of heat treatment. The degree of the reaction between the molten Cu–Ni–Mn–Fe alloys and W–C particulate could be limited by controlling the iron content of the binders to obtain an optimal interface.

Keywords: metal matrix composites, spontaneous infiltration, interfacial reactions, precipitation-hardening matrix, microhardness

1. Introduction

Metal matrix composites (MMCs) are advanced materials displaying improved strength, a superior resistance to wear and corrosion and a high temperature stability making them suitable for a wide range of industrial applications [1, 2]. Over recent decades, many new composites have been developed, some with very valuable properties [3–5]. By carefully choosing the reinforcement, the matrix, and the manufacturing process that brings them together, engineers can tailor the properties to meet specific requirements. To fabricate MMCs with enhanced properties, the processing technique must ensure a high volume fraction of reinforcement, its uniform distribution and acceptable adhesion between the matrix and the reinforcing phase without unwanted interfacial reactions that degrade the mechanical properties. Many processing techniques have been developed to produce MMCs employing a variety of binder and reinforcement combinations [6–12]. Among these, a spontaneous infiltration process is widely used for making MMCs with a high volume fraction of reinforcements which offers many more advantages compared to those of other conventional manufacturing processes [13–16].

The reinforcement, the matrix and the interface between them determine the characteristics of MMCs. Particles of various materials are currently used as reinforcement [17–24]. The size of particles varies from millimetres to nano levels. Even though various kinds of composites have been developed, among them tungsten carbides as reinforcement particles have proven to be promising materials because of their excellent mechanical properties coupled with a good tribological performance [25–28].

In terms of high-temperature strength properties, copper-matrix composites are superior compared with other MMCs [29–32]. Commercial copper alloys usually contain manganese, nickel and iron to improve performance characteristics [33–37]. The cast materials have a high fluidity and can reproduce fine details in master patterns during infiltration, while their good corrosion and oxidation resistance promotes longer service life. The high strength of the Cu–Ni–Mn–Fe alloys is attained by precipitation hardening [37–42]. This process involves the formation of θ-NiMn phase from a supersaturated solid solution of alpha-copper. The evolution of NiMn precipitates dispersed in the α-Cu matrix affects the achievement of the material's final strength [37, 40].

Although the precipitation hardening of the Cu–Ni–Mn–Fe alloys may allow wear resistance and mechanical strength desired in special applications of the composite materials, no information has been found in the literature concerning the usage of Cu–Ni–Mn–Fe alloys as binders of MMCs reinforced by the W–C particulate which are prepared by the infiltration process. The processing to produce MMC materials and components commonly involves high temperatures. During such processing, the high reactivity of the molten binder often leads to the production of thick interfacial layers, which tend to be defective and brittle. These usually embrittle and weaken the composites, with the interface having a very important influence on their properties. Hence, the understanding of the mechanism of interfacial reactions during infiltration is of significant importance in controlling the microstructural and mechanical properties of MMCs [43, 44]. This allows the properties of MMCs to be tailored to applications requiring a combination of high-performance characteristics. Therefore, in this work the mechanism of the interfacial reactions was analyzed to obtain a theoretical and experimental basis for the preparation of (Cu–Ni–Mn–Fe)/(W–C) particulate composites with improved overall properties.

2. Materials and methods

The (Cu–Ni–Mn–Fe)/(W–C) particulate composites were made by a spontaneous infiltration process, in which tungsten carbides with an average particle size of about 0.2–1.5 mm were penetrated by a molten Cu–Ni–Mn–Fe binder metal, which filled the space between the filler particles [14]. The used W–C filler, containing C (3.5–3.7 wt.%) and W – the remainder, had a eutectic ($WC+W_2C$) structure. The investigated Cu–Ni–Mn–Fe binders were prepared in the following compositional ranges (purity better than 99.9%): Ni (19.3–21.0 wt.%), Mn (19.5–20.5 wt.%), Fe (0–2.35 wt.%) and Cu – the remainder. Infiltration process parameters were as follows: infiltration temperature 1050°C and infiltration time 30 min. The quality of infiltration was subsequently investigated by optical microscopy (NEOPHOT-2), quantitative metallography (EPIQUANT), scanning electron microscopy (JEOL-2010 F) and energy-dispersive X-ray spectroscopy (EDX).

The wetting properties of Cu–Ni–Mn–Fe alloys were evaluated for W–C substrates to determine their viability for the production of MMCs via spontaneous infiltration. This was accomplished through the use of sessile drop experiments at a typical processing temperature of 1050°C in vacuum [45]. The uncertainty of the measured contact angles did not exceed ±1°.

To investigate the precipitation hardening of Cu–Ni–Mn–Fe matrix, the MMCs samples were annealed at 900°C for 60 and 750 h and then cooled in water to preserve their structure. Annealing under these conditions for 750 h was assumed to be equivalent to a 3-year service life at 500°C [46]. Microhardness (H_μ) was measured by a PMT-3 *Vickers* indenter. Measurements were done by using 0.196 and 0.49 N loads at room temperature. The loading and unloading times were 10 s each.

3. Results and discussion

The initial contact angle of Cu–Ni–Mn alloy on the W–C substrate was 30°, and the final contact angle was 3°. The molten metal continued to spread across the surface throughout the experiment. The Cu–Ni–Mn–Fe alloys had initial contact angles of 20–25°, decreasing with increasing the iron content, and the final contact angle was 0°, which means that the metal fully spreads across the surface of the W–C substrate. So, iron has no negative effect on the wettability of the W–C substrate by the Cu–Ni–Mn–Fe alloys, and these alloys may be used as binder materials for MMCs.

Through the spontaneous infiltration process, (Cu–Ni–Mn–Fe)/(W–C) composite materials with more than 55 vol.% reinforcement and a low porosity (~2%) were successfully fabricated. The porosity decreased by 3–4 times when iron was added to the Cu–Ni–Mn binder. This decrease in porosity can be attributed to the role of Fe in enhancing the wettability between the Cu–Ni–Mn–Fe binders and W–C particles. The microstructure of the infiltrated composites was mainly composed of the reinforcement phase (W–C particles) with a bright contrast and the matrix phase (Cu–Ni–Mn–Fe alloy) with a grey contrast (Fig. 1). The final MMCs had a homogenous distribution of the reinforcement phase which usually ensures enhanced performance properties and prolonged service life [14]. The W–C particles retained their initial shape and surface morphology.

The matrix/filler interfaces were examined to determine if there were reactions at the interface to effectively control physical-and-chemical processes between the Cu–Ni–Mn–Fe molten binders and the W–C particulate at infiltration temperature. Figure 1 presents the micrographs of the (Cu–Ni–Mn–Fe)/(W–C) composites depending on the iron content of the binder that show no evidence of interfacial delamination, debonding or other defects, which are detrimental to the mechanical properties of MMCs. The investigated interfaces are marked by a 14–17 μm thick continuous layer between the particulate and the matrix. The light phase in the layer at the interface was determined by EDX to be W_2C carbide (Fig. 1(a)). There is also evidence of separate W_2C inclusions in the copper-based matrix (Fig. 1(b, c)). The W_2C carbides at the interfaces can be an evidence of the preferential dissolution of WC carbide of the eutectic (WC+W_2C) filler during infiltration.

EDX was also used to determine how the matrix segregated around the interface. When wetted with the Cu–Ni–Mn–Fe binder, the diffusion of tungsten (up to ~0.94 wt.%) and carbon (up to ~0.04 wt.%) from the W–C filler towards the matrix and the counter diffusion of nickel (up to ~1.22 wt.%) and iron (up to ~0.34 wt.%) from the matrix towards the filler occur. A noticeable penetration of copper and manganese atoms from the Cu–Ni–Mn–Fe matrix into the particulate is not revealed by EDX. The thickness of the W_2C layer at the interfaces increases as the iron content of the Cu–Ni–Mn–Fe binder is raised up to 1.75 wt.% (Table 1). However, a higher addition of Fe has little effect on the thickness of the interfacial layers.

The Cu–Ni–Mn–Fe matrix of MMCs shows no evidence of secondary compound formation. But interfacial reactions cause the changes in the microhardness values due to the dissolution and diffusion processes. As a result, the microhardness of the filler near the interface decreases but the microhardness of the matrix increases. Examples of these changes are shown in Fig. 2, which demonstrates how the microhardness of MMCs increases as the iron content of the Cu–Ni–Mn–Fe binders increases.

The sequence of physical-and-chemical processes occurring at the studied MMCs interfaces can be represented as follows. When wetting filler particles with the molten binder, the less stable WC

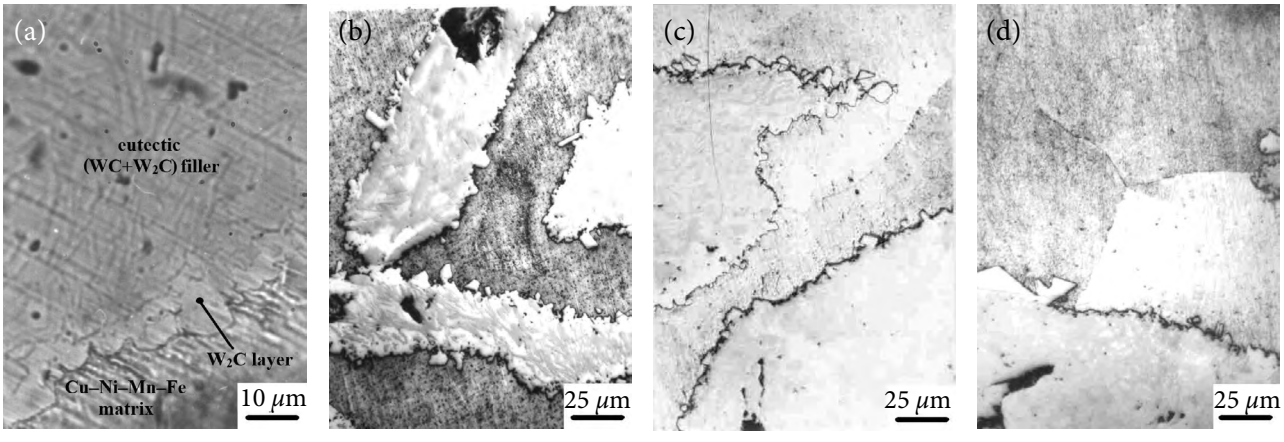

Fig. 1. Micrographs of MMCs infiltrated by binders: (a) Cu–20.5% Ni–20% Mn–0.6% Fe; (b) Cu–21% Ni–20.5% Mn–1.75% Fe; (c) Cu–20% Ni–19.5% Mn–2.1% Fe; (d) Cu–20.5% Ni–19.5% Mn–2.35% Fe.

Table 1. An average thickness (in μm) of the interfacial layer between the W–C filler and the Cu–Ni–Mn–Fe matrices of MMCs.

Binder	Before annealing	After annealing at 900°C	
		for 60 h	for 750 h
Cu–20% Ni–20% Mn	2.1±1.0	8.0±1.5	9.0±1.5
Cu–20.5% Ni–20% Mn–0.6% Fe	14.1±1.0	25.0±1.5	32.0±1.5
Cu–21% Ni–20.5% Mn–1.75% Fe	17.3±0.8	32.5±1.0	33.5±1.0
Cu–20% Ni–19.5% Mn–2.1% Fe	17.2±1.1	31.3±1.0	34.1±1.0
Cu–20.5% Ni–19.5% Mn–2.35% Fe	17.4±1.7	32.0±1.5	35.0±1.5

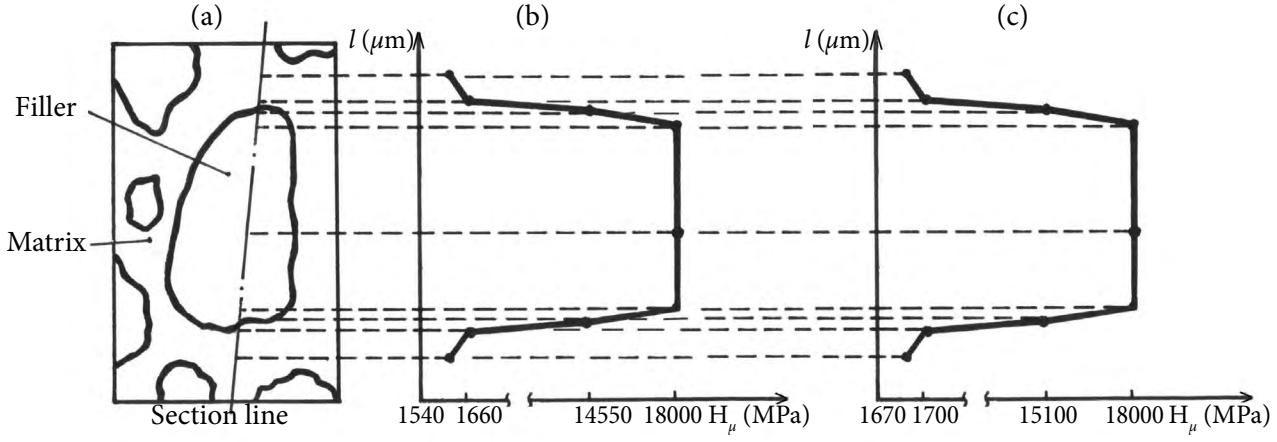

Fig. 2. The microhardness profiles across the (Cu–Ni–Mn–Fe)/(W–C) composites: (a) schematic of MMC; (b) Cu–20.5% Ni–20% Mn–0.6% Fe binder; (c) Cu–20.5% Ni–19.5% Mn–2.35% Fe binder.

phase of the eutectic (WC+W_2C) filler dissolves at a higher rate. The dissolution stage is preceded by the predominant penetration of iron atoms from the molten Cu–Ni–Mn–Fe binder into this phase (Table 2). Diffusion of iron atoms from the molten metal into the W_2C filler phase is much lower (Fig. 3). This carbide dissolves at a relatively slow rate, and after infiltration the W_2C layer and/or separate W_2C inclusions are seen between the particulate and the matrix. The formation of the W_2C interfacial layer is connected mainly with the one-way diffusion of Fe atoms from the Cu–Ni–Mn–Fe matrix towards the WC phase. Diffusing Ni atoms are distributed almost uniformly in both filler phases and may influence their dissolution rates presumably in the same way (Table 2).

In the early stage, the interfacial layer is very thin, thus, the Fe atoms may diffuse more easily than during the later stage. Besides, as the iron content of the binder is increased up to 1.75 wt.%, the W_2C layer thickness increases, thereby lengthening the diffusion path of Fe atoms through the layer and resulting in a decreased dissolution rate. This implies that the WC filler phase can dissolve at a higher rate when there is a supply of iron atoms from the matrix. Therefore, as the iron content is

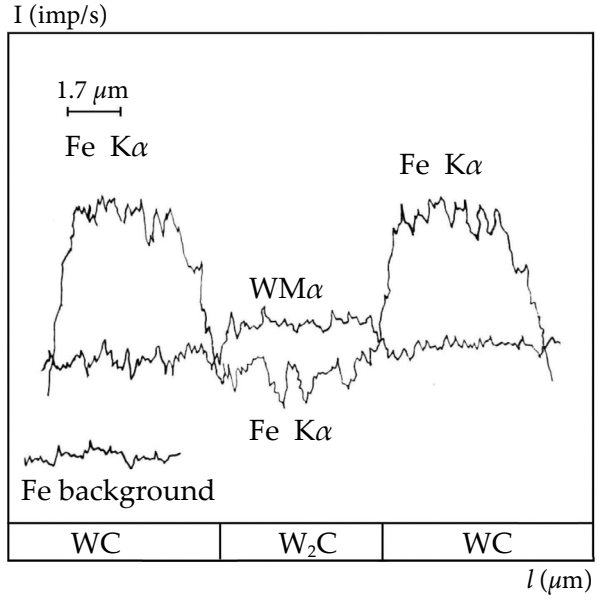

Fig. 3. The EDX profiles of Fe and W across the eutectic (WC+W_2C) filler near the (Cu–Ni–Mn–Fe)/(W–C) interface.

Table 2. Content of Fe and Ni (in wt.%) diffusing from the Cu–Ni–Mn–Fe matrix into the W–C filler near the interface.

Matrix	Filler phases			
	WC		W_2C	
	Fe	Ni	Fe	Ni
Cu–20.5% Ni–20% Mn–0.6% Fe	0.12	1.07	0.05	1.16
Cu–21% Ni–20.5% Mn–1.75% Fe	0.33	1.11	0.07	1.22
Cu–20% Ni–19.5% Mn–2.1% Fe	0.32	1.08	0.06	1.19
Cu–20.5% Ni–19.5% Mn–2.35% Fe	0.34	1.12	0.05	1.17

further raised up to 2.1 wt.% and higher, the thickness of interfacial layer remains almost unchanged. Hence, the study shows that a layer of W_2C, which forms at the interface and retards further dissolution processes, is responsible for the limited interfacial reactions observed in this composite system.

It is worth noting that the described processes are typical of the dissolution-and-diffusion mechanism of the interface formation which ensures a strong interfacial bond between the reinforcing particles and the metal matrix. The interfacial reactions result in the layer of W_2C carbide at the interface, with coefficient of thermal expansion about 2 times higher than that of WC carbide [47], and so its value is closer to the value for the copper-based matrix [48]. So, any cracking upon cooling from the processing temperature to the room temperature because of different coefficients of thermal expansion becomes less possible. This means that the W–C particles and Cu–Ni–Mn–Fe matrix have a good compatibility and excellent wetting characteristics with each other. So, iron has a much stronger positive effect on optimizing the (Cu–Ni–Mn–Fe)/(W–C) interface binding and inhibits harmful interfacial reactions.

The optical images of MMCs after annealing at 900°C for 60 and 750 h are shown in Figs. 4 and 5. After annealing, the interfaces are similar in that there are a layer and/or inclusions of W_2C carbide between the Cu–Ni–Mn–Fe matrix and the W–C filler. As in the as-prepared condition, additions of up to 1.75 wt.% of iron to the binder metal increase the thickness of W_2C layer at the interface by promoting the dissolution of WC filler phase (Table 1). The higher iron content is, the thicker interfacial W_2C layer forms that ensures the interface bonding and enhances the quality of the composites. But, increasing the Fe content above 1.75 wt.% does not lead to noticeable changes in the thickness of W_2C layer. However, during annealing, the diffusion rate of Fe atoms increases as compared with that during infiltration, so the formed interfacial layer becomes relatively thick. The effect tends to be more marked after the first 60 h of annealing. This indicates that the diffusion-controlled dissolution processes with further prolonged annealing time slow down and

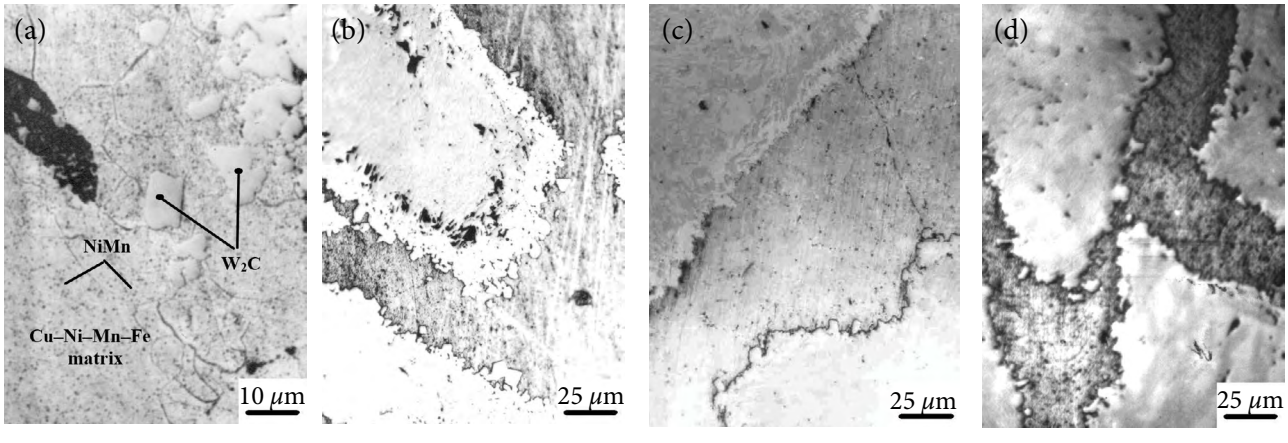

Fig. 4. Micrographs of MMCs annealed at 900°C for 60 h with binders: (a) Cu–20.5% Ni–20% Mn–0.6% Fe; (b) Cu–21% Ni–20.5% Mn–1.75% Fe; (c) Cu–20% Ni–19.5% Mn–2.1% Fe; (d) Cu–20.5% Ni–19.5% Mn–2.35% Fe.

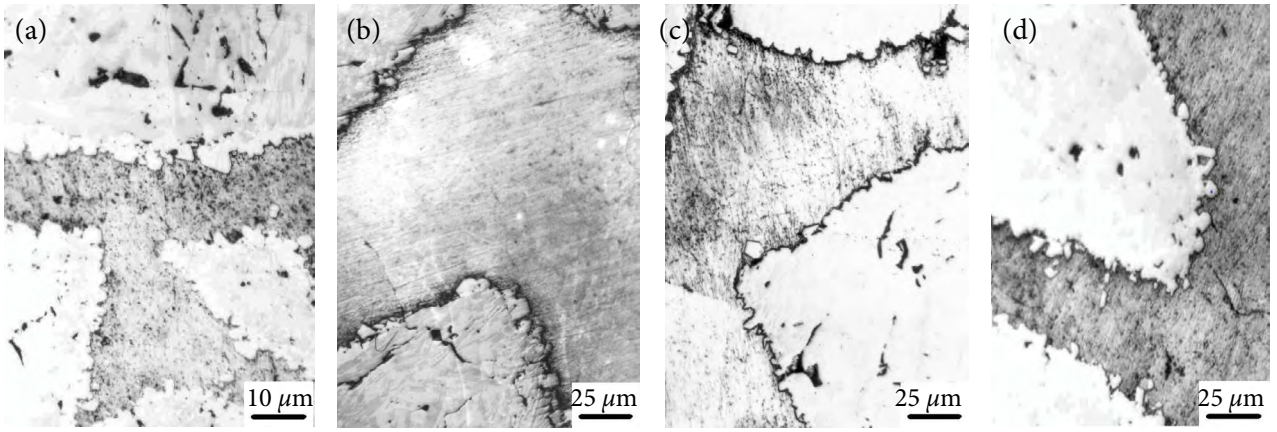

Fig. 5. Micrographs of MMCs annealed at 900°C for 750 h with binders: (a) Cu–20.5% Ni–20% Mn–0.6% Fe; (b) Cu–21% Ni–20.5% Mn–1.75% Fe; (c) Cu–20% Ni–19.5% Mn–2.1% Fe; (d) Cu–20.5% Ni–19.5% Mn–2.35% Fe.

stabilize due to reaching quasi-equilibrium conditions at the interface.

At the same time, it has been noticed that after annealing in the structure of the Cu–Ni–Mn–Fe matrix appear the fine precipitates of the NiMn phase of dark colour (Figs. 4, 5). They are formed both at the grain boundaries and throughout the matrix α-copper solution. An average size of precipitates ranges from 3 to 5 μm. Longer annealing time leads to higher values of the volume fraction of the NiMn phase. Thus, for MMCs with the Cu–21% Ni–20.5% Mn–1.75% Fe binder, the fraction of NiMn precipitates amounts to 12±3 vol.% after 60-hour annealing, and it is 28±3 vol.% after 750-hour annealing. As the iron content of the Cu–Ni–Mn–Fe binder is raised from 0.6 to 2.35 wt.%, the volume fraction of the NiMn phase slightly increases after annealing at 900°C for 60 h (by ~5–6 vol.%) and does not noticeably change after annealing for 750 h. So, iron is more beneficial for obtaining precipitated phases during the first 60 h of annealing [37].

As shown in Table 3, the measurements of microhardness near the interface evidence that iron present in the binder functions in two ways: one is to enhance diffusion and dissolution processes at the interfaces and the other is to accelerate the ageing of the Cu–Ni–Mn–Fe matrix during annealing. Considering that the precipitation hardening of the Cu–Ni–Mn–Fe matrix ensures the wear resistance and mechanical strength of MMCs [25], additions of up to 2.35 wt.% of iron to Cu–Ni–Mn binders have a positive effect.

Thus, iron added to Cu–Ni–Mn infiltrating binders for particulate composites is found advantageous in promoting not only the formation of a binding W_2C layer at the interface between the W–C particles and the Cu–Ni–Mn–Fe matrix but also the precipitation of NiMn as a dispersed phase within the α-copper matrix.

4. Conclusions

In this work, (Cu–Ni–Mn–Fe)/(W–C) particulate composites prepared by the spontaneous infiltration technique have been characterized for interfacial reactions between the infiltrating binders and the filler. With relevance to characterization, the composites have been found to be non-porous

Table 3. Microhardness (in GPa) of the (Cu–Ni–Mn–Fe)/(W–C) MMCs after annealing at 900°C for 750 h.

Binder	Matrix		Filler	
	away from the interface	near the interface	away from the interface	near the interface
Cu–20.5% Ni–20% Mn–0.6% Fe	1.31±0.15	1.58±0.2	17.0±0.3	13.9±0.1
Cu–21% Ni–20.5% Mn–1.75% Fe	1.40±0.2	1.69±0.1	18.2±0.4	15.0±0.3
Cu–20% Ni–19.5% Mn–2.1% Fe	1.42±0.3	1.52±0.4	17.9±0.1	14.9±0.2
Cu–20.5% Ni–19.5% Mn–2.35% Fe	1.45±0.2	1.51±0.14	18.0±0.2	15.1±0.6

and microscopically homogeneous in the distribution of W–C particles.

Cu–Ni–Mn–Fe binders show favourable interfacial properties with final contact angles of 0°, making them viable candidates for spontaneous infiltration. The wetting properties of Cu–Ni–Mn–Fe binders are found to improve with a higher iron content of the alloys. The physical-and-chemical processes at the (Cu–Ni–Mn–Fe)/(W–C) interface involve the diffusion of both W and C outwards as well as Ni and Fe inwards, while other elements hardly diffuse through the reaction zone. There is evidence that Fe from Cu–Ni–Mn–Fe binders penetrates mainly into the WC phase of eutectic (WC+W_2C) fillers, which causes its rapid dissolution. The contribution of Ni diffusion through the reaction products to the WC dissolution process is relatively small. As a result, W–C particles react with the Cu–Ni–Mn–Fe infiltrating alloys to form a W_2C layer at the interface and dissolve tungsten and carbon of mainly the WC phase into the molten metal binder. The W_2C layer at the reaction interface between the Cu–Ni–Mn–Fe alloys and the W–C particulate does not inhibit further wetting in applications such as infiltration. The thickness of this layer increases when the iron content of the Cu–Ni–Mn–Fe binders is raised up to 1.75 wt.%, indicating that the interfacial reactions reach the quasi-equilibrium at higher iron content and may be effectively controlled by binder composition.

Iron present in the Cu–Ni–Mn–Fe binders not only promotes wetting by intensifying interfacial reactions between the particulate and the matrix but also accelerates processes of precipitation hardening helping in the strengthening of the matrix alloy in the (Cu–Ni–Mn–Fe)/(W–C) particulate composites. And so, compared to that for the other three components of the Cu–Ni–Mn–Fe binders, the iron content was more influential to changes in the structure of the studied MMCs.

References

[1] N. Chawla and K.K. Chawla, *Metal Matrix Composites* (Springer, New York, 2013), https://doi.org/10.1007/978-1-4614-9548-2

[2] S. Suresh, A. Mortensen, and A. Needleman, *Fundamentals of Metal-Matrix Composites* (Butterworth-Heinemann, Stoneham, 2013).

[3] K.U. Kainer, in: *Metal Matrix Composites. Custom-made Materials for Automotive and Aerospace Engineering*, ed. K.U. Kainer (Wiley-VCH Verlag, Weinheim, 2006) pp. 1–54.

[4] Y.G. Chabak, V.I. Fedun, K. Shimizu, V.G. Efremenko, and V.I. Zurnadzhy, Phase-structural composition of coating obtained by pulsed plasma treatment using eroded cathode of T1 high speed steel, Probl. At. Sci. Technol. **104**(4), 100–106 (2016).

[5] J.B. Ferguson, B.F. Schultz, and P.K. Rohatgi, Self-healing metals and metal matrix composites, JOM **66**(6), 866–871 (2014), https://doi.org/10.1007/s11837-014-0912-4

[6] Z.A. Duryagina, S.A. Bespalov, A.K. Borysyuk, and V.Ya. Pidkova, Magnetometric analysis of surface layers of 12X18H10T steel after ion-beam nitriding, Metallofiz. Noveishie Tekhnol. **33**(5), 615–622 (2011), https://doi.org/10.1007/s11003-012-9514-x

[7] Y.L. Ivanytskyj, T.M. Lenkovskiy, Y.V. Molkov, V.V. Kulyk, and Z.A. Duriagina, Influence of 65G steel microstructure on crack faces friction factor under mode II fatigue fracture, Arch. Mater. Sci. Eng. **82**(2), 49–56 (2016), https://doi.org/10.5604/01.3001.0009.7103

[8] S.I. Ryabtsev, V.A. Polonskyy, and O.V. Sukhova, Structure and corrosion of quasicrystalline cast alloys and Al–Cu–Fe film coatings, Mater. Sci. **56**(2), 263–272 (2020), https://doi.org/10.1007/s11003-020-00428-8

[9] I.M. Spiridonova, E.V. Sukhovaya, V.F. Butenko, A.P. Zhudra, A.I. Litvinenko, and A.I. Belyi, Structure and properties of boron-bearing iron granules for composites, Powder Metall. Met. Ceram. **32**(2), 139–141 (1993), https://doi.org/10.1007/BF00560039

[10] R. Tkachenko, Z. Duriagina, I. Lemishka, I. Izonin, and A. Trostianchyn, Development of machine learning method of titanium alloy properties identification in additive technologies, East.-Eur. J. Enterp. Technol. **3**(12–93), 23–31 (2018), https://doi.org/10.15587/1729-4061.2018.134319

[11] O.V. Sukhova, Structure and properties of Fe–B–C powders alloyed with Cr, V, Mo or Nb for plasma-sprayed coatings, Probl. At. Sci. Technol. **4**(128),

77–83 (2020), https://doi.org/10.46813/2020-128-077

[12] Y. Chabak, V. Efremenko, V. Zurnadzhy, V. Puchý, I. Petryshynets, B. Efremenko, V. Fedun, K. Shimizu, I. Bogomol, V. Kulyk, and D. Jakubéczyová, Structural and tribological studies of "(TiC + WC)/hardened steel" PMMC coating deposited by air pulsed plasma, Metals **12**, 218 (2022), https://doi.org/10.3390/met12020218

[13] P.M. Brune, *Processing and Properties of WC-based Cu–Ni–Mn–Zn Metal Matrix Composites Produced via Pressureless Infiltration*, Masters Theses, 7850 (2017), https://scholarsmine.mst.edu/masters_theses/7850

[14] E.V. Sukhovaya, Structural approach to the development of wear-resistant composite materials, J. Superhard Mater. **35**(5), 277–283 (2013), https://doi.org/10.3103/S106345761305002X

[15] O.V. Sukhova and Yu.V. Syrovatko, New metallic materials and synthetic metals, Metallofiz. Noveishie Tekhnol. **41**(9), 1171–1185 (2019), https://doi.org/10.15407/mfint.41.09.1171

[16] I. Daoud, Dj. Miroud, and R. Yamanoglu, Microstructure characterization and quantitative analysis of copper alloy matrix composites reinforced with WC-xNi powders prepared by spontaneous infiltration, J. Min. Metall. B **54**(2), 169–177 (2018), https://doi.org/10.2298/JMMB171225005D

[17] O.V. Sukhova, V.A. Polonskyy, and K.V. Ustinova, Corrosion-electrochemical properties of quasicrystalline Al–Cu–Fe–(Si,B) and Al–Ni–Fe alloys in NaCl solution, Vopr. Khimii Khimicheskoi Tekhnologii **124**(3), 46–52 (2019) [in Ukrainian], https://doi.org/10.32434/0321-4095-2019-124-3-46-52

[18] B.O. Trembach, M.G. Sukov, V.A. Vynar, I.O. Trembach, V.V. Subbotina, O.Yu. Rebrov, O.M. Rebrova, and V.I. Zakiev, Effect of incomplete replacement of Cr for Cu in the deposited alloy of Fe–C–Cr–B–Ti alloying system with a medium boron content (0.5% wt.) on its corrosion resistance, Metallofiz. Noveishie Tekhnol. **44**(4), 493–513 (2022), https://doi.org/10.15407/mfint.44.04.0493

[19] R. Babilas, A. Bajorek, M. Spilka, A. Radon, and W. Lonski, Structure and corrosion resistance of Al–Cu–Fe alloys, Prog. Nat. Sci. **30**(3), 393–401 (2020), https://doi.org/10.1016/j.pnsc.2020.06.002

[20] O.V. Sukhova, The effect of carbon content and cooling rate on the structure of boron-rich Fe–B–C alloys, Phys. Chem. Solid State **21**(2), 355–360 (2020), https://doi.org/10.15330/pcss.21.2.355-360

[21] H. Wang, Z.-H. Zhang, Z.-Y. Hu, Q. Song, S.-P. Yin, Z. Kang, and S.-L. Li, Improvement of interfacial interaction and mechanical properties in copper matrix composites reinforced with copper coated carbon nanotubes, Mater. Sci. Eng. A **715**, 163–173 (2018), https://doi.org/10.1016/j.msea.2018.01.005

[22] O.V. Sukhova, V.A. Polonskyy, and K.V. Ustinova, Structure formation and corrosion behaviour of quasicrystalline Al–Ni–Fe alloys, Phys. Chem. Solid State **18**(2), 222–227 (2017), https://doi.org/10.15330/PCSS.18.2.222-227

[23] K. Młynarek-Żak, A. Wierzbicka-Miernik, M. Kądziołka-Gaweł, T. Czeppe, A. Radoń, and R. Babilas, Electrochemical characterization of rapidly solidified Al–(Cr,Cu,Ni,Y,Zr)–Fe alloys, Electrochim. Acta **409**, 139836 (2022), https://doi.org/10.1016/j.electacta.2022.139836

[24] O.V. Sukhova and V.A. Polonskyy, Structure and corrosion of quasicrystalline cast Al–Co–Ni and Al–Fe–Ni alloys in aqueous NaCl solution, East Eur. J. Phys. **3**, 5–10 (2020), https://doi.org/10.26565/2312-4334-2020-3-01

[25] J. Liu, S. Yang, W. Xia, X. Jiang, and Ch. Gui, Microstructure and wear resistance performance of Cu–Ni–Mn alloy based hardfacing coatings reinforced by WC particles, J. Alloys Compd. **654**, 63–70 (2015), https://doi.org/10.1016/j.jallcom.2015.09.130

[26] A.V. Muller, D. Ewert, A. Galatanu, M. Milwich, R. Neu, J.Y. Pastor. U. Siefken, E. Tejado, and J.H. You, Melt infiltrated tungsten–copper composites as advanced heat sink materials for plasma facing components of future nuclear fusion devices, Fusion Eng. Des. **124**,

455–459 (2017), https://doi.org/10.1016/j.fusengdes.2017.01.042

[27] V. Jankauskas, M. Antonov, V. Varnauskas, R. Skirkus, and D. Goljandin, Effect of WC grain size and content on low stress abrasive wear of manual arc welded hardfacing with low-carbon or stainless steel matrix, Wear **328–329**, 378–390 (2015), https://doi.org/10.1016/j.wear.2015.02.063

[28] M. Jäcklein, A. Pfaff, and K. Hoschke, Developing tungsten-filled metal matrix composite materials using laser powder bed fusion, Appl. Sci. **10**(24), 8869 (2020), https://doi.org/10.3390/app10248869

[29] *Copper Alloys: Preparation, Properties and Applications*, eds. M. Naboka and J. Giordano, (Nova Science Publishers Inc., Hauppauge, N. Y., 2011).

[30] M. Schutze, R. Feser, and R. Bender, *Corrosion Resistance of Copper and Copper Alloy*s (Wiley-VCH, Weinheim, 2011).

[31] B. Trembach, A. Grin, V. Subbotina, V. Vynar, S. Knyazev, V. Vakiev, I. Trembach, and O. Kabatskyi, Effect of exothermic addition (CuO–Al) on the structure, mechanical properties and abrasive wear resistance of the deposited metal during self-shielded flux-cored arc welding, Tribol. Ind. **43**(3), 452–464 (2021), https://doi.org/10.24874/ti.1104.05.21.07

[32] O.V. Sukhova, Solubility of Cu, Ni, Mn in boron-rich Fe–B–C alloys, Phys. Chem. Solid State **22**(1), 110–116 (2021), https://doi.org/10.15330/pcss.22.1.110-116

[33] P. Sakiewicz, R. Nowosielski, and R. Babilas, Production aspects of inhomogeneous hot deformation in as-cast CuNi25 alloy, Indian J. Eng. Mater. Sci. **22**(4), 389–398 (2015).

[34] R. Wang, Y. Fu, G. Xie, Z. Hao, S. Zhang, and X. Liu, The microstructure and mechanical properties of Cu–20Ni–20Mn alloy fabricated by a compact preparation process, Metals **10**, 1528–1537 (2020), https://doi.org/10.3390/met10111528

[35] B. Trembach, A. Grin, N. Makarenko, S. Zharikov, I. Trembach, and O. Markov, Influence of the core filler composition on the recovery of alloying elements during the self-shielded flux-cored arc welding, J. Mater. Res. Technol. **9**(5), 10520–10528 (2020), https://doi.org/10.1016/j.jmrt.2020.07.052

[36] S. Sharma, X.N. Dong, P. Wei, and C. Long, Electro-chemical deposited Cu–Ni binary and Cu–Ni–Mn ternary alloys from sulphate bath for anti-corrosive coating applications in brine environment: Effect of corrosion behaviour, polarization studies, morphological and structural characterizations, Key Eng. Mater. **837**, 102–108 (2020), https://doi.org/10.4028/www.scientific.net/KEM.837.102

[37] O.V. Sukhova, The effect of iron on precipitation hardening in the Cu–Ni–Mn alloys, Phys. Chem. Solid State **22**(3), 487–493 (2021), https://doi.org/10.15330/pcss.22.3.487–493

[38] H. Kang, Z. Yang, X. Yang, J. Li, W. He, Z. Chen, E. Guo, L.-D. Zhao, and T. Wang, Preparing bulk Cu–Ni–Mn based thermoelectric alloys and synergistically improving their thermoelectric and mechanical properties using nanotwins and nanoprecipitates, Mater. Today Phys. **17**, 100332 (2020), https://doi.org/10.1016/j.mtphys.2020.100332

[39] W. Xie, Q. Wang, X. Mi, G. Xie, D. Liu, X. Gao, and Y. Li, Microstructure evolution and properties of Cu–20Ni–20Mn alloy during aging process, Trans. Nonferrous Met. Soc. China **25**(10), 3247–3251 (2015), https://doi.org/10.1016/s1003-6326(15)63960-7

[40] J. Zou, L. Shi, H. Shi, Q. Feng, and S. Liang, Study on aging strengthening and nano precipitates of Cu–Ni–Mn–Fe alloy, Mater. Res. Express **7**, 056504 (2020), https://doi.org/10.1088/2053-1591/ab8bld

[41] S. Reeh, D. Music, M. Ekholm, I. Abrikosov, and J.M. Schneider, Elastic properties of fcc Fe–Mn–*X*(*X*=Cr, Co, Ni, Cu) alloys from first-principles calculations, Phys. Rev. B. **87**, 224103 (2013), https://doi.org/10.1103/PhysRevB.87.224103

[42] S. Hocker, P. Binkele, and S. Schmauder, Precipitation in α-Fe based Fe–Cu–Ni–Mn-alloys: behaviour of Ni and Mn modelled by ab initio and kinetic Monte Carlo simulations, Appl. Phys. Res. **115**(2), 679–687 (2014), https://doi.org/10.1007/s00339-013-7850-9

[43] R.Y. Lin, Composite interfacial reactions, JOM **45**, 20 (1993), https://doi.org/10.1007/BF03222343

[44] A.I. Mertens and J. Lecomte-Beckers, in: *New Trends in 3D Printing*, ed. I.V. Shishkovsky (Intech, Liege, 2016) pp. 187–213, https://doi.org/10.5772/63045

[45] Yu.M. Ivashchenko and V.N. Eremenko, *Basics of Precise Measurement of Surface Energy by Sessile Drop Method* (Naukova dumka, Kyiv, 1972) [in Russian].

[46] C.J. Smithells, *Metal Reference Book* (Butterworth & Co., London-Boston, 1976).

[47] T.Ya. Kosolapova, *Properties, Preparation and Application of Refractory Compounds* (Metallurgy, Moscow, 1986) [in Russian].

[48] L.N. Larikov and Yu.F. Yurchenko, *Thermal Properties of Metals and Alloys* (Naukova dumka, Kyiv, 1985) [in Russian].

FIZIKINIAI IR CHEMINIAI VYKSMAI (Cu–Ni–Mn–Fe)/(W–C) KOMPOZITŲ SANDŪROJE

O.V. Sukhova

Olesio Gončiaro vardo Dnipro nacionalinio universiteto Fizikos, elektronikos ir kompiuterių sistemų fakultetas, Dnipras, Ukraina